

# Mechanism and Rate Constants for the Reactions of Cl Atoms with HOCl, CH<sub>3</sub>OCl and *tert*-C<sub>4</sub>H<sub>9</sub>OCl

A. Kukui, J. Roggenbuck, and R. N. Schindler

Institut für Physikalische Chemie der Universität Kiel, Ludewig-Meyn-Straße 8, D-24098 Kiel, Germany

*Key Words:* Chemical Kinetics / Elementary Reactions / Mass Spectrometry / Radicals

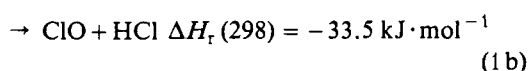
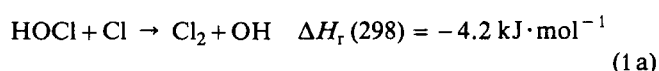
Reactions of Cl atoms with HOCl (1), CH<sub>3</sub>OCl (2) and C<sub>4</sub>H<sub>9</sub>OCl (3) have been investigated at 300 K using discharge flow LIF/MS technique. The mechanism and reaction rate constants were determined by monitoring absolute rates of hypochlorite and Cl atom consumption together with the build-up of reaction products. Based on the yields of Cl<sub>2</sub> and OH in (1a), Cl<sub>2</sub> and CH<sub>3</sub>O in (2a) and Cl<sub>2</sub> in (3a), as measured by MS/LIF, the reactions of Cl atom with the hypochlorites investigated in this work were found to proceed predominantly via the Cl atom abstraction channel with  $k_{1a}/k_1 = (0.96 \pm 0.05)$ ,  $k_{2a}/k_2 = (0.85 \pm 0.06)$ ,  $k_{3a}/k_3 = (1.01 \pm 0.05)$ .



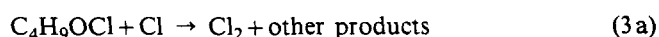
The reaction rate constants were determined to be  $k_1 = (2.28 \pm 0.09) \cdot 10^{-12}$ ,  $k_2 = (6.0 \pm 0.2) \cdot 10^{-11}$ , and  $k_3 = (4.26 \pm 0.2) \cdot 10^{-11}$ , all in units  $\text{cm}^3 \cdot \text{molecule}^{-1} \cdot \text{s}^{-1}$ . A reevaluation of the heat of formation of HOCl yielded  $\Delta H_f^\circ(298 \text{ K}) = -75.1 \text{ kJ} \cdot \text{mol}^{-1}$ .

## Introduction

Hypochlorous acid (HOCl) is known to be an important atmospheric reservoir for active chlorine and thus acts as an intermediate promoting ozone depletion in the polar stratosphere [1]. The significance of this reservoir in stratospheric ozone chemistry is determined mainly by its photolytic decomposition and by its heterogeneous reactions with HCl [2]. In addition, the mechanism of HOCl reaction with Cl atoms, O atoms or with OH radicals is of interest for modelling purposes because two abstraction channels (1a) and (1b) are thermodynamically available to the Cl atoms



Analogous reaction channels are possible for reactions of methyl hypochlorite (CH<sub>3</sub>OCl) and *tert*-butyl hypochlorite (C<sub>4</sub>H<sub>9</sub>OCl) with Cl.



CH<sub>3</sub>OCl has been identified as a product in the reaction of ClO with methylperoxy radicals [3] and therefore might participate in methane oxidation processes relevant to stratospheric chemistry [4]. To estimate the importance of

reaction (2) compared to the photolysis of CH<sub>3</sub>OCl [5] the rate constant as well as the mechanism of reaction (2) are of interest.

Here we present results of a MS/LIF study on the kinetics and product formation in the reactions of Cl atoms with HOCl, CH<sub>3</sub>OCl and C<sub>4</sub>H<sub>9</sub>OCl. The primary focus of this investigation was the mechanism of the above reactions which appear to proceed mainly via the Cl abstraction channel. An investigation of the reaction of OH radicals with hypochlorites shall be presented in an upcoming contribution [6].

## Experimental

In the present investigation the discharge fast flow reactor was coupled to a combined laser induced fluorescence/mass-spectrometric (LIF/MS) detection system. The experimental set-up has been described elsewhere [7, 8]. The reactor consisted of a 36 mm i.d., 400 mm long quartz flow tube and a movable inlet which was a Pyrex tube of 15 mm i.d. Both tubes had side arms, each equipped with inlet ports and microwave cavities for F or Cl generation. Ceramic (Al<sub>2</sub>O<sub>3</sub>) insets were used in the discharge region. Inner surfaces of the reactor were coated with Halocarbon wax. Flow velocities of He were in the range 5–19 m s<sup>-1</sup> at total pressures of 2.5–3.5 mbar of He. The temperature was 300 ± 3 K.

Chlorine atoms were produced in the movable inlet using the fast reaction  $\text{F} + \text{HCl} \rightarrow \text{HF} + \text{Cl}$  in excess of HCl, or by passing Cl<sub>2</sub>/He mixtures through a microwave discharge. Cl and Cl<sub>2</sub> were registered by MS on 35 and 70/72 amu, respectively, at electron energies of 15 eV. Calibration of Cl signals was performed using the titration reaction (4)



OH and CH<sub>3</sub>O radicals were monitored by LIF using the  $A^2\Sigma^+ \leftarrow X^2\Pi$  transition of OH and the  $A^2A_1 \leftarrow X^2E$  transition of CH<sub>3</sub>O at wavelengths of 306.505 and 303.9 nm, respectively [9, 10]. Details for the LIF detection system have been presented in [7]. Calibration of the OH LIF signal was performed using reaction (5) by measuring the corresponding consumption of NO<sub>2</sub> and the OH radical yields.



H atoms were prepared inside the injector using reaction  $\text{F} + \text{H}_2 \rightarrow \text{HF} + \text{H}$  in an excess of H<sub>2</sub>. NO<sub>2</sub> was added into the flow tube via the side arm of the reactor.

HOCl has been prepared as aqueous solution using the procedure described in [11, 12] and transported into the reactor through the side arm of the flow tube by bubbling He carrier gas through the HOCl solution at a temperature of about 0–5°C. The concentration of HOCl was controlled by MS on the parent ion signal 52 amu at 15 eV electron energy. Calibration of HOCl MS signals was performed measuring absolute concentration yields of HOCl from the reaction of OH radicals produced in the injector via (5) with an excess of Cl<sub>2</sub> [13]



In the different experiments [HOCl] varied in the range  $2 \cdot 10^{12} - 2.5 \cdot 10^{13}$  molecule·cm<sup>-3</sup>. Typical concentrations of H<sub>2</sub>O in the reactor were  $(1 - 10) \cdot 10^{14}$  molecule·cm<sup>-3</sup>.

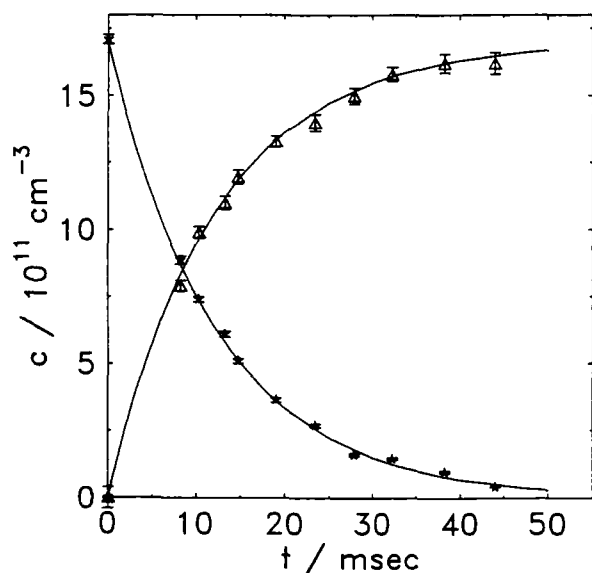


Fig. 1  
Reaction  $\text{HOCl} + \text{Cl} \rightarrow \text{Cl}_2 + \text{OH}$ . Typical profiles for the decay of HOCl (\*) and generation of Cl<sub>2</sub> (Δ) at  $[\text{Cl}]_0 = 3.3 \cdot 10^{13}$  and  $[\text{HOCl}]_0 = 1.7 \cdot 10^{12}$ , in units molecule cm<sup>-3</sup>. The Cl atoms were generated in reaction  $\text{F} + \text{HCl} \rightarrow \text{HF} + \text{Cl}$ . The solid lines are the results of a numerical simulation using  $k_1 = 2.5 \cdot 10^{-12}$  cm<sup>3</sup>·molecule<sup>-1</sup>·s<sup>-1</sup> (cf. Table 1)

Methyl hypochlorite CH<sub>3</sub>OCl and *tert*-butyl hypochlorite C<sub>4</sub>H<sub>9</sub>OCl were prepared as described in [14] and [15], respectively. Details shall be presented in [6].

## Results

### 1. The Reaction HOCl + Cl

The reaction of HOCl with Cl atoms (1) has been investigated by monitoring decay profiles of HOCl in an excess of Cl and the build-up of OH and Cl<sub>2</sub> which were the only products of (1) observed in this work. In determinations of Cl<sub>2</sub> yields the reaction  $\text{F} + \text{HCl}$  has been employed to generate Cl atoms. The background MS signal on 70 amu in these experiments constituted typically (0.1–1%) of the Cl<sub>2</sub> signals produced in reaction (1a). In order to avoid an interference from the relatively fast reaction of OH radicals with HCl, the measurement of OH yields in (1a) was performed by passing Cl<sub>2</sub>/He mixture through the microwave discharge to generate Cl atoms. Typical profiles for the decay of HOCl and the formation of Cl<sub>2</sub> and OH are presented in Figs. 1 and 2, respectively.

Formation of ClO radicals via reaction channel (1b) could not be detected in any of these experiments. The mass-spectrometric signal on 51 amu corresponding to ClO radicals was independent of reaction time and sufficiently low to neglect a possible interference from Cl<sub>2</sub>O [11].

The overall reaction constant  $k_1 = (2.28 \pm 0.09) \cdot 10^{-12}$  cm<sup>3</sup>·molecule<sup>-1</sup>·s<sup>-1</sup> was determined by simulating HOCl profiles taking the reactions (6), (7) and (8) into account with rate constants  $k_6 = 6.83 \cdot 10^{-14}$  [13],  $k_7 = 1.88 \cdot 10^{-12}$

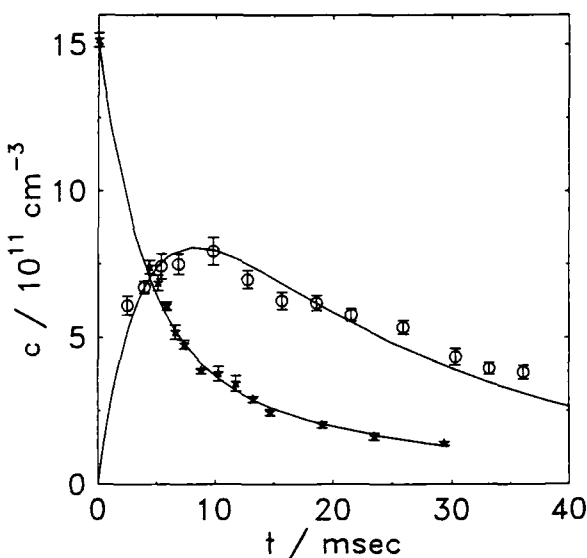


Fig. 2  
Reaction  $\text{HOCl} + \text{Cl} \rightarrow \text{Cl}_2 + \text{OH}$ . Typical profiles for the decay of HOCl (\*) and generation of OH (○) at  $[\text{Cl}]_0 = 7 \cdot 10^{13}$  and  $[\text{HOCl}]_0 = 1.5 \cdot 10^{12}$ , in units molecule cm<sup>-3</sup>. The solid lines are the results of a numerical simulation using  $k_1 = 2.13 \cdot 10^{-12}$  cm<sup>3</sup>·molecule<sup>-1</sup>·s<sup>-1</sup> (cf. Table 1). Note that Cl-atoms were generated in these experiments by passing Cl<sub>2</sub> through a discharge, thus enabling regeneration of HOCl through step (6)

[16] and  $k_8 = 7.93 \cdot 10^{-13}$  [16], in units  $\text{cm}^3 \cdot \text{molecule}^{-1} \cdot \text{s}^{-1}$ .



Self reaction of OH radicals was significant only in experiments in which the initial concentration of HOCl was sufficiently high (see Table 1). Regeneration of HOCl in reaction (6) is obvious from the [HOCl] shape as presented in Fig. 2 and thus indicates formation of OH radicals via (1a). Wall loss of OH radicals varied in the range  $(5 - 20) \text{ s}^{-1}$  depending on the concentrations of Cl<sub>2</sub> and H<sub>2</sub>O and was determined in separate experiments. Experimental conditions and derived reaction rate constants are summarized in Table 1.

Branching ratios  $k_{1a}/k_1$  were evaluated by fitting calculated reaction time dependencies of [OH] and [Cl<sub>2</sub>] to the experimentally obtained build-up profiles with the value for  $k_{1a}/k_1$  being the only variable. Rate constants  $k_1$  used in the fitting were taken from the simulation of HOCl profiles obtained in the same experimental runs. As shown in Figs. 1 and 2 for OH and Cl<sub>2</sub>, respectively, the behaviour of experimental OH and Cl<sub>2</sub> profiles can be adequately described with the same rate parameters as the experimental HOCl profiles. Note, that branching ratios found with this procedure from yields of OH radicals are sensitive only to the relative mass spectrometric sensitivities for OH and HOCl which have been measured directly through the consumption and generation of OH and HOCl, respectively, in the reaction of OH with Cl<sub>2</sub>. The average for  $k_{1a}/k_1$  is  $(0.96 \pm 0.05)$ . Together with the absence of ClO formation this clearly indicates predominance of channel (1a), i.e. the abstraction of Cl atom from HOCl.

Table 1  
Rate constants and branching ratios for the reactions HOCl + Cl (1), CH<sub>3</sub>OCl + Cl (2) and C<sub>4</sub>H<sub>9</sub>OCl + Cl (3)

Reaction HOCl + Cl			
[Cl] <sub>0</sub> , 10 <sup>13</sup> molecule cm <sup>-3</sup>	[HOCl] <sub>0</sub> , 10 <sup>12</sup> molecule cm <sup>-3</sup>	k <sub>1</sub> , 10 <sup>-12</sup> cm <sup>3</sup> · molecule <sup>-1</sup> · s <sup>-1</sup>	k <sub>1a</sub> /k <sub>1</sub>
5.1 <sup>a)</sup>	25	2.44 ± 0.4	1.05 ± 0.1 <sup>a)</sup>
2.6 <sup>a)</sup>	25	2.31 ± 0.4	0.88 ± 0.1 <sup>a)</sup>
1.9 <sup>a)</sup>	8.7	2.74 ± 0.3	0.89 ± 0.1 <sup>a)</sup>
7.03 <sup>a)</sup>	1.5	2.13 ± 0.2	1.14 ± 0.2 <sup>a)</sup>
7.03 <sup>a)</sup>	0.63	2.19 ± 0.2	1.08 ± 0.2 <sup>a)</sup>
3.4 <sup>a)</sup>	0.19	2.27 ± 0.3	0.95 ± 0.2 <sup>a)</sup>
5.3 <sup>b)</sup>	2.6	2.11 ± 0.3	0.91 ± 0.2 <sup>b)</sup>
3.3 <sup>b)</sup>	2.6	2.43 ± 0.3	0.98 ± 0.2 <sup>b)</sup>
5.35 <sup>b)</sup>	1.74	2.05 ± 0.3	0.81 ± 0.2 <sup>b)</sup>
3.3 <sup>b)</sup>	1.7	2.51 ± 0.3	1.05 ± 0.2 <sup>b)</sup>
Reaction CH <sub>3</sub> OCl + Cl			
[CH <sub>3</sub> OCl] <sub>0</sub> , 10 <sup>12</sup> molecule cm <sup>-3</sup>	[Cl] <sub>0</sub> , 10 <sup>11</sup> molecule cm <sup>-3</sup>	k <sub>2</sub> <sup>c)</sup> , 10 <sup>-11</sup> cm <sup>3</sup> · molecule <sup>-1</sup> · s <sup>-1</sup>	k <sub>2a</sub> /k <sub>2</sub> <sup>d)</sup>
5.5	15	4.4 ± 0.4	0.81 ± 0.1
5.5	4.1	6.4 ± 0.3	0.85 ± 0.1
5.5	2.3	5.8 ± 0.4	0.89 ± 0.2
8.8	4.5	6.1 ± 0.4	0.86 ± 0.2
11.4	2.3	6.5 ± 0.3	0.89 ± 0.2
13.5	4.5	6.1 ± 0.4	0.89 ± 0.3
Reaction C <sub>4</sub> H <sub>9</sub> OCl + Cl			
[C <sub>4</sub> H <sub>9</sub> OCl] <sub>0</sub> , 10 <sup>12</sup> molecule cm <sup>-3</sup>	[Cl] <sub>0</sub> , 10 <sup>11</sup> molecule cm <sup>-3</sup>	k <sub>3</sub> <sup>c)</sup> , 10 <sup>-11</sup> cm <sup>3</sup> · molecule <sup>-1</sup> · s <sup>-1</sup>	k <sub>3a</sub> /k <sub>3</sub> <sup>d)</sup>
73	22.2	–	1.12 ± 0.1
69	17.3	–	1.00 ± 0.1
14.1	12.2	–	0.96 ± 0.1
15.0	5.34	4.2 ± 0.3	0.85 ± 0.2
5.95	1.14	4.2 ± 0.3	1.05 ± 0.2
3.5	1.11	4.4 ± 0.4	0.96 ± 0.3

<sup>a)</sup> Experiments with Cl atoms produced by dissociation of Cl<sub>2</sub> and with branching ratio  $k_{1a}/k_1$  determined from the yields of OH radicals.

<sup>b)</sup> Experiments with Cl atoms produced in the reaction F + HCl and with branching ratio  $k_{1a}/k_1$  determined from the yields of Cl<sub>2</sub>.

<sup>c)</sup> Determined from the decay rates of Cl atoms.

<sup>d)</sup> Determined from the absolute yields of Cl<sub>2</sub>.

## 2. The Reaction CH<sub>3</sub>OCl + Cl

The reaction of Cl atoms with methyl hypochlorite has been investigated in an excess of [CH<sub>3</sub>OCl] = (0.55 – 13.5) · 10<sup>12</sup> molecule cm<sup>-3</sup> monitoring the time dependence of the Cl signal decay together with the formation of Cl<sub>2</sub> and CH<sub>3</sub>O. Typical concentration profiles are presented in Fig. 3. The mean value  $k_2 = (6.0 \pm 0.2) \cdot 10^{-11}$  cm<sup>3</sup> · molecule<sup>-1</sup> · s<sup>-1</sup> has been calculated using the individual data presented in Table 1, which have been derived from the simulation of Cl atom decay profiles.

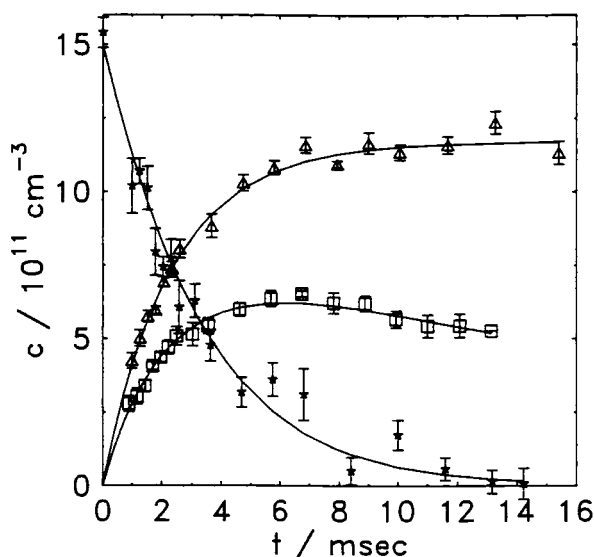


Fig. 3  
Reaction CH<sub>3</sub>OCl + Cl → Cl<sub>2</sub> + CH<sub>3</sub>O. Typical profiles for the decay of Cl (\*) and the generation of Cl<sub>2</sub> (△) and CH<sub>3</sub>O (□) at [Cl]<sub>0</sub> = 1.5 · 10<sup>12</sup> and [CH<sub>3</sub>OCl]<sub>0</sub> = 5.5 · 10<sup>12</sup>, in units molecule cm<sup>-3</sup>. The solid lines are the results of a numerical simulation using  $k_2 = 4.4 \cdot 10^{-11}$  cm<sup>3</sup> · molecule<sup>-1</sup> · s<sup>-1</sup> (cf. Table 1). For [CH<sub>3</sub>O] no calibration was available

The calculated time dependence for Cl<sub>2</sub> formation was based on step (2a) being the predominant primary step in the system. The alternative H abstraction by Cl attack to yield CH<sub>2</sub>OCl followed by the secondary reaction of Cl with this intermediate to yield Cl<sub>2</sub> has also been included in the model. According to these calculations formation of Cl<sub>2</sub> along this pathway is negligible. Under experimental conditions of Fig. 3 the yield of Cl<sub>2</sub> from this route constitutes to only about 3%, assuming on rate constant of  $2 \cdot 10^{-10}$  cm<sup>3</sup> · molecule<sup>-1</sup> · s<sup>-1</sup> for the reaction Cl + CH<sub>2</sub>OCl → Cl<sub>2</sub> + CH<sub>2</sub>O.

For the evaluation of the branching ratio  $k_{2a}/k_2$  build-up profiles of Cl<sub>2</sub> were simulated with the values for  $k_{2a}/k_2$  being the variable. Rate constants were taken from the corresponding Cl profiles measured under the same experimental conditions. The average value of  $k_{2a}/k_2 = (0.85 \pm 0.06)$  indicates predominance of the Cl abstraction reaction channel in (2). This result is in agreement with the observed changes in methoxy radical concentrations shown in Fig. 3. The time dependences of [CH<sub>3</sub>O] can be described with rate con-

stants derived from Cl atom decay rates. Also, the observed dependencies of methoxy LIF signals on the initial Cl concentrations were in agreement with the results of simulations. Direct measurements of absolute CH<sub>3</sub>O yields were not performed in this work.

The most significant process included in the reaction scheme used for the simulation was the secondary reaction (9) of Cl with CH<sub>3</sub>O with  $k_9 = 1 \cdot 10^{-10}$  cm<sup>3</sup> · molecule<sup>-1</sup> · s<sup>-1</sup> [7].



Variation of  $k_9$  from our previously measured value  $k_9 = 1 \cdot 10^{-10}$  to  $k_9 = 1.8 \cdot 10^{-11}$  cm<sup>3</sup> · molecule<sup>-1</sup> · s<sup>-1</sup> [17] would lead to an about 10% increase of the derived rate constant  $k_2$  and to a ~10% decrease of  $k_{2a}/k_2$  values.

## 3. The Reaction CH<sub>4</sub>O<sub>9</sub>Cl + Cl

The experimental approach to the investigation of reaction (3) was analogous to that used for study of reaction (2). Experiments were carried out in an excess of C<sub>4</sub>H<sub>9</sub>OCl over Cl atoms, (see Table 1). The overall reaction constant  $k_3$  and the branching ratio  $k_{3a}/k_3$  were derived simulating decay profiles for [Cl] and formation profiles for [Cl<sub>2</sub>]. Molecular chlorine was the only primary product observed in these experiments. Average values  $k_3 = (4.26 \pm 0.2) \cdot 10^{-12}$  cm<sup>3</sup> · molecule<sup>-1</sup> · s<sup>-1</sup> and  $k_{3a}/k_3 = (1.01 \pm 0.05)$  were obtained from the data presented in Table 1.

## Discussion

The results of previous investigations on the kinetics of the reaction of HOCl with Cl [11, 18, 19] are in good agreement with the value  $k_1 = (2.28 \pm 0.09) \cdot 10^{-12}$  cm<sup>3</sup> · molecule<sup>-1</sup> · s<sup>-1</sup> obtained in this work. However, the result on the branching ratio  $k_{1a}/k_1 = (0.96 \pm 0.05)$  as determined in the present investigation, which is within experimental uncertainty in agreement with  $(0.91 \pm 0.06)$  published by Ennis and Birks [20], is at variance with  $(0.24 \pm 0.11)$  as reported before from this laboratory [11]. The reason for this serious discrepancy must be related to the calibration procedure for HOCl applied in the previous investigation, which was based on a titration with F atoms. As have been pointed out in [11] the HOCl source employed had contained various amounts of H<sub>2</sub>O and Cl<sub>2</sub>O depending on the temperature of the cooling trap installed between HOCl reservoir and reactor tube. The complexity of the system towards F atoms has apparently caused an underestimation of the experimental sensitivity for HOCl as compared with Cl<sub>2</sub>. The branching ratio reported in [11] should thus be superseded by the value obtained in the present study, which is based on reaction (6) relating HOCl formation to OH consumption.

With the new value for the experimental HOCl sensitivity, which differs from the previously reported value by a factor of 4 also the branching ratios for the reactions (10) and (11) investigated in [11]



must be corrected to  $k_{10\text{a}}/k_{10} \cong 1$  and  $k_{11\text{a}}/k_{11} \cong 0.8$ .

According to the results of this work reaction pair (1a) and (6) constitutes a system of reversible reactions and thus the equilibrium constant  $K_{\text{eq}}$  (298) = 34.03 can be recalculated with the rate constant  $k_1 = 2.28 \cdot 10^{-12} \text{ cm}^3 \cdot \text{molecule}^{-1} \cdot \text{s}^{-1}$  and the constant  $k_6 = 6.7 \cdot 10^{-14} \text{ cm}^3 \cdot \text{molecule}^{-1} \cdot \text{s}^{-1}$  as reported by Loewenstein and Anderson [18]. This leads with  $\Delta G_r^0 = -RT \ln K_{\text{eq}} = -8.74 \text{ kJ} \cdot \text{mol}^{-1}$  and through the Gibbs-Helmholtz relation to a reaction enthalpy of  $\Delta H_r^0 = -7.2 \text{ kJ} \cdot \text{mol}^{-1}$ . From this the heat of formation  $\Delta H_f^0(\text{HOCl}) = -75.1 \text{ kJ} \cdot \text{mol}^{-1}$  at 298 K is derived. All standard entropies and enthalpies of formation data for the calculations were taken from JANAF Thermochemical Tables [21]. This value for the heat of formation of HOCl is lower than the earlier estimated value of  $-79.7 \text{ kJ} \cdot \text{mol}^{-1}$  [11] but is in good agreement with  $\Delta H_f^0(\text{HOCl})$  recommended in the NASA Evaluation Panel [22], in the JANAF Thermochemical Tables [21] (see [23] for further references) and a most recent evaluation based on photoionization efficiency spectra of Cl<sub>2</sub>O [28].

Branching ratios for the reactions of Cl with CH<sub>3</sub>OCl and with C<sub>4</sub>H<sub>9</sub>OCl were obtained by following [Cl<sub>2</sub>] formation and the consumption of [Cl] atoms. These measurements were based on the relative sensitivities for Cl and Cl<sub>2</sub> derived directly from reaction (4). The values  $k_{2\text{a}}/k_2 = (0.85 \pm 0.06)$  and  $k_{3\text{a}}/k_3 = (1.01 \pm 0.05)$  obtained in this work are surprising, but the value for reaction (2) is in good agreement with preliminary results of Crowley et al. [24]. According to our data reaction channels other than Cl atom abstraction in CH<sub>3</sub>OCl may account for about 15% of reaction (2). Although formation of HCl or CH<sub>2</sub>OCl could not be unambiguously established in our experiments, this does not exclude the possibility of H atom abstraction. Accurate monitoring of HCl was hampered in the system through the Cl atom source and, on the other hand, the MS sensitivity for CH<sub>2</sub>OCl may be very low. It should be pointed out that also in reactions of F-atoms with alkyloxychlorides not the intuitively expected H abstraction is the predominant pathway. With HOCl nearly exclusive FCl formation is obtained. Comparable results were also obtained with alkyloxychlorides [6].

## Conclusions

The results obtained in this investigation provide unambiguous evidence that the reactions of Cl atoms with alkyl hypochlorites proceed predominantly via Cl abstraction to yield Cl<sub>2</sub>. This result is surprising since reactions of Cl atoms with alkanes, haloalkanes, alcohols and with other organic molecules are known to proceed by H abstraction

only and they are known to be very fast. It is suggested that special bonding properties in the alkyloxyhalide/halogen atom interacting couple are responsible for this peculiarity. Mechanistically the reaction of Cl atoms with hypochlorites can be compared with the reaction of O(<sup>3</sup>P) atoms with HOCl, in which the primary attack of the O atoms occurred at the Cl site of HOCl [25]. For the thermodynamically identical attack of O(<sup>3</sup>P) at the hydrogen in HOCl a high activation barrier has been estimated using ab-initio model calculations [25]. Also in reactions of F atoms with hypochlorites a preferred formation of ClF has been observed [6]. Finally, in the reaction of OH radicals with a series of alkyl hypochlorites also the Cl abstraction reaction prevails [6].

The behaviour of HOCl is analogous to that of HOBr, for which the attack of O(<sup>3</sup>P) and Cl(<sup>2</sup>P) was found to occur at the halogen only [26], in contradiction to statements reported by others [27].

The work described in this paper was supported within the CEC-Programme "Environment" and within the Ozonforschungsprogramm of the BMBF, Bonn.

## References

- [1] Scientific Assessment of Ozone Depletion, WMO Global Ozone Research Monitoring Project, Report 37 (1995).
- [2] J. P. D. Abbat and M. J. Molina, *Geophys. Res. Lett.* **19**, 461 (1992).
- [3] R. D. Kenner, K. R. Ryan, and I. C. Plumb, *Geophys. Res. Lett.* **20**, 1571 (1993); F. Helleis, J. N. Crowley, and G. K. Moortgat, *J. Phys. Chem.* **97**, 11464 (1993); A. S. Kukui, T. P. W. Jungkamp, and R. N. Schindler, *Ber. Bunsenges. Phys. Chem.* **98**, 1298 (1994); F. Helleis, J. N. Crowley, and G. K. Moortgat, *Geophys. Res. Lett.* **21**, 1795 (1994).
- [4] P. J. Crutzen, R. Müller, C. Brühl, and T. Peter, *Geophys. Res. Lett.* **19**, 1113 (1992).
- [5] R. N. Schindler, M. Liesner, S. Schmidt, U. Kirchner, and Th. Benter, *J. Photochem. Photobiol. A Chemistry*, in press (1997).
- [6] A. Kukui, J. Roggenbuck, and R. N. Schindler, to be submitted.
- [7] T. P. W. Jungkamp, A. Kukui, and R. N. Schindler, *Ber. Bunsenges. Phys. Chem.* **99**, 1057 (1995).
- [8] E. Becker, U. Wille, M. M. Rahman, and R. N. Schindler, *Ber. Bunsenges. Phys. Chem.* **95**, 1173 (1991).
- [9] G. Herzberg, *Spectra of Diatomic Molecules*, D. Van Nostrand Company, New York 1966.
- [10] G. Inoue, H. Akimoto, and M. Okuda, *J. Chem. Phys.* **72**, 1769 (1980).
- [11] R. Vogt and R. N. Schindler, *Ber. Bunsenges. Phys. Chem.* **97**, 819 (1993).
- [12] T. Permien, R. Vogt, and R. N. Schindler, in: *Mechanismus of Gas Phase and Liquid Phase Chemical Transformations*, ed. by R. A. Cos, *Air Pollution Report 17*, 149 (1988).
- [13] W. B. DeMore, D. M. Golden, R. F. Hampson, C. J. Howard, M. J. Kurilo, M. J. Molina, A. R. Ravishankara, S. P. Sander, *Chemical kinetics and photochemical data for use in stratospheric modeling*. JPL Publication 87-41, Jet Prop. Lab., Pasadena CA 1987.
- [14] T. Sandmeyer, *Ber. Dtsch. Chem. Ges.* **19**, 859 (1886).
- [15] M. J. Mintz and C. Walling, *Org. Synth. Coll.*, Vol. V, 186 (1973).
- [16] R. Atkinson, D. L. Baulch, R. A. Cox, R. F. Hampson Jr., J. A. Kerr, and J. Troe, *J. Phys. Chem. Ref. Data* **21**, 1125 (1992).
- [17] V. Daele, G. Laverdet, and G. Poulet, *Int. J. Chem. Kinet.* **28**, 589 (1996).

- [18] L.M. Loewenstein, J.G. Anderson, *J. Phys. Chem.* **88**, 6277 (1984).
- [19] Jac-E.L. Cook, C.A. Ennis, T.J. Leck, and J.W. Birks, *J. Chem. Phys.* **74**, 545 (1981).
- [20] C.A. Ennis and J.W. Birks, *J. Phys. Chem.* **89**, 186 (1985).
- [21] M.W. Chase Jr., C.A. Davies, J.R. Downey Jr., D.J. Frurip, R.A. McDonald, and A.N. Syverud, *J. Phys. Chem. Ref. Data* **14**, Suppl. JANAF Thermochemical Tables (1985).
- [22] W.B. DeMore, S.P. Sander, D.M. Golden, R.F. Hampson, M.J. Kurylo, C.J. Howard, A.B. Rawishankara, C.E. Kolb, and M.J. Molina, *Chemical Kinetics and Photochemical Data for Use in Stratospheric Modeling*, JPL Publication, 90-1, Jet Propulsion Laboratory, Pasadena, California 1992.
- [23] R.P. Wayne, G. Poulet, P. Biggs, J.P. Burrows, R.A. Cox, P.J. Crutzen, G.D. Hayman, M.E. Jenkin, G. Le Bras, G.K. Moortgat, U. Platt, and R.N. Schindler, *Atmospheric Environment* **29**, 2677 (1995).
- [24] J.N. Crowley, P. Campuzano-Jost, and G.K. Moortgat, *J. Phys. Chem.* **100**, 3601 (1996).
- [25] R.N. Schindler, J. Dethlefs, and M. Schmidt, *Ber. Bunsenges. Phys. Chem.* **100**, 1242 (1996).
- [26] A. Kukui, U. Kirchner, Th. Benter, and R.N. Schindler, *Ber. Bunsenges. Phys. Chem.* **100**, 455 (1996).
- [27] P.S. Monks, F.L. Nesbitt, M. Scanlon, and L.J. Stief, *J. Phys. Chem.* **97**, 11699 (1993).
- [28] R. Peyton Thorn Jr., L.J. Stief, Szu-Cherng Kuo, and R. Bruce Klemm, *J. Phys. Chem.* **100**, 14178 (1996).

(Received: August 16, 1996

E 9355

final version: November 18, 1996)